

MAASTRICHTIAN TO YPRESIAN SLOPE-BASIN DEPOSITS OF THE ULTRAHELVETIC NAPPE COMPLEX (ACHTHAL FORMATION)

Hans Egger, Omar Mohamed

Topics:

Cretaceous-Paleogene transition in an active tectonic deep-water setting. Slope basin formation on the bathyal to abyssal southern slope of the European Plate.

Tectonic unit:

Ultrahelvetic nappe complex

Lithostratigraphic units:

Buntmergelserie, Achthal Formation (type locality)

Chronostratigraphic units:

Upper Maastrichtian to Lower Eocene

Biostratigraphic units:

Calcareous nannoplankton zones CC26 to NP11

Location:

Stecherwald southwest of Teisendorf (Bavaria)

Coordinates:

Base of the section: E 012° 47' 42", N 47° 50' 51"; Top of the section: E 012° 48' 02", N 47° 50' 48"

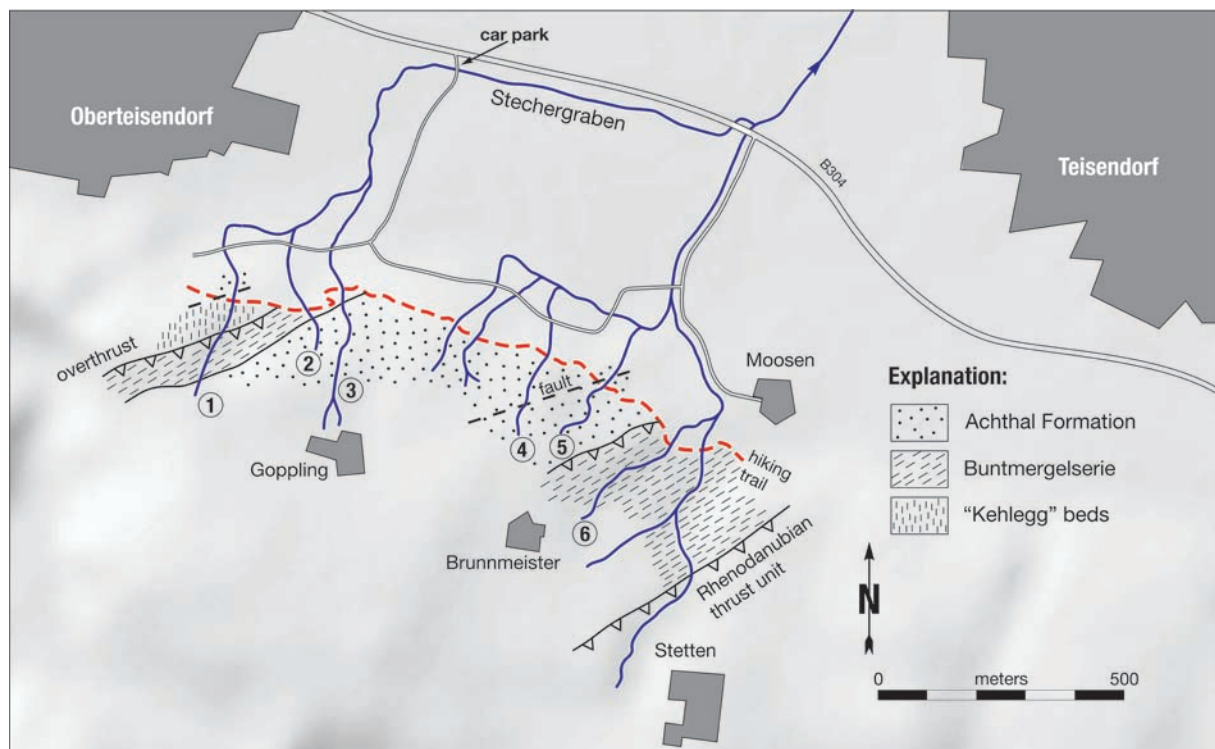
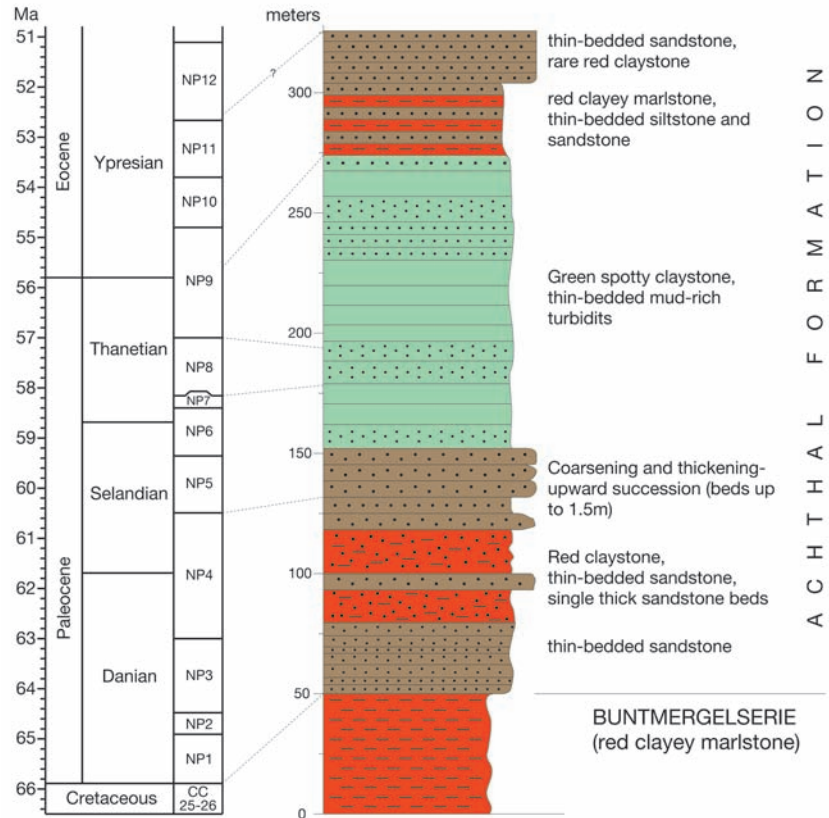


Figure A2.21 ▲

Sketch map of the area investigated. Numbers indicate the most important creek sections mentioned in the text.

Figure A2.22 ►
Composite log of the Achthal Formation in the type area (Stecherwald near Teisendorf).



The type area of the Achthal Formation is the forest (“Stecherwald”) southwest of Teisendorf. The base of the composite type section of the Achthal Formation (Goppling section) is located in creek 3 (“Gopplingbach”), ca. 15 m south of the hiking trail bridge. Further up-stream the Danian, Selandian and lower Thanetian all show excellent exposures, which end at the hamlet of Goppling. The upper Thanetian is seen only in small and poor exposures, in the two gullies east of creek 3 (Fig. A2.21). The Eocene part of the section is well exposed along creek 4, with the first outcrop ca. 20 m downstream from the hiking trail.

The lithostratigraphic term “Achthaler Sandstein” dates back to Gümbel (1862, p.616). Although Schlosser (1925, p.167) mentioned a Thanetian macrofauna from this unit (“Achthaler Grünsand”), it can be assumed that these fossils originated from the tectonically neighbouring shallow-water deposits of the south-Helvetic thrust unit. Ganss and Knipscheer (1956) report on Paleocene foraminifera faunas and interpreted the outcrops as a special facies (Teisendorf facies) of the Helvetic sedimentation area. Hagn (1960 and 1967) recognized the deep-water character of the deposits and assigned them to the southern part of the Ultrahelvetic sedimentation area, which interpretation is adopted by Egger & Mohamed (2010), who introduced the term “Achthal Formation” for the deep-water turbidite succession.

The base of the Achthal Formation, which conformably overlies the Buntmergelserie, is defined by the onset of turbiditic sedimentation in the uppermost Maastrichtian. The stratigraphic top is unknown because of the tectonic truncation of the Goppling section. However, deposition of the Achthal Formation probably ended in the Ypresian because grey calcareous marlstone of early Lutetian age occurs in the Ultrahelvetic thrust unit at Mattsee in Austria (Rögl and Egger, 2010 – STOPA2/1), only ca. 25 km northeast of Teisendorf.

Figure A2.23 ►

Sedimentary facies at the Goppling section. **1** Buntmergelserie, Upper Maastrichtian (CC25), creek 3; **2** Sandstone beds of lower Danian age, creek 3; **3** and **4** Danian sandstone and intervening red claystone, creek 3; **5** The highest red claystone layers, upper Danian (NP3-4), creek 3. Note the flute casts at the base of the sandstone indicating paleotransport parallel to the trend of the strike; **6** Thick-bedded sandstone, Selandian (NP5); **7** Mud-rich facies with abundant bioturbated green hemipelagic claystone and thin turbiditic sandstone. Note the erosional channels perpendicular to the trend of the strike (Selandian-Thaletian), creek 3; **8** Bioturbated red marlstone and thin-bedded silt turbidites, Ypresian (NP11), creek 4.



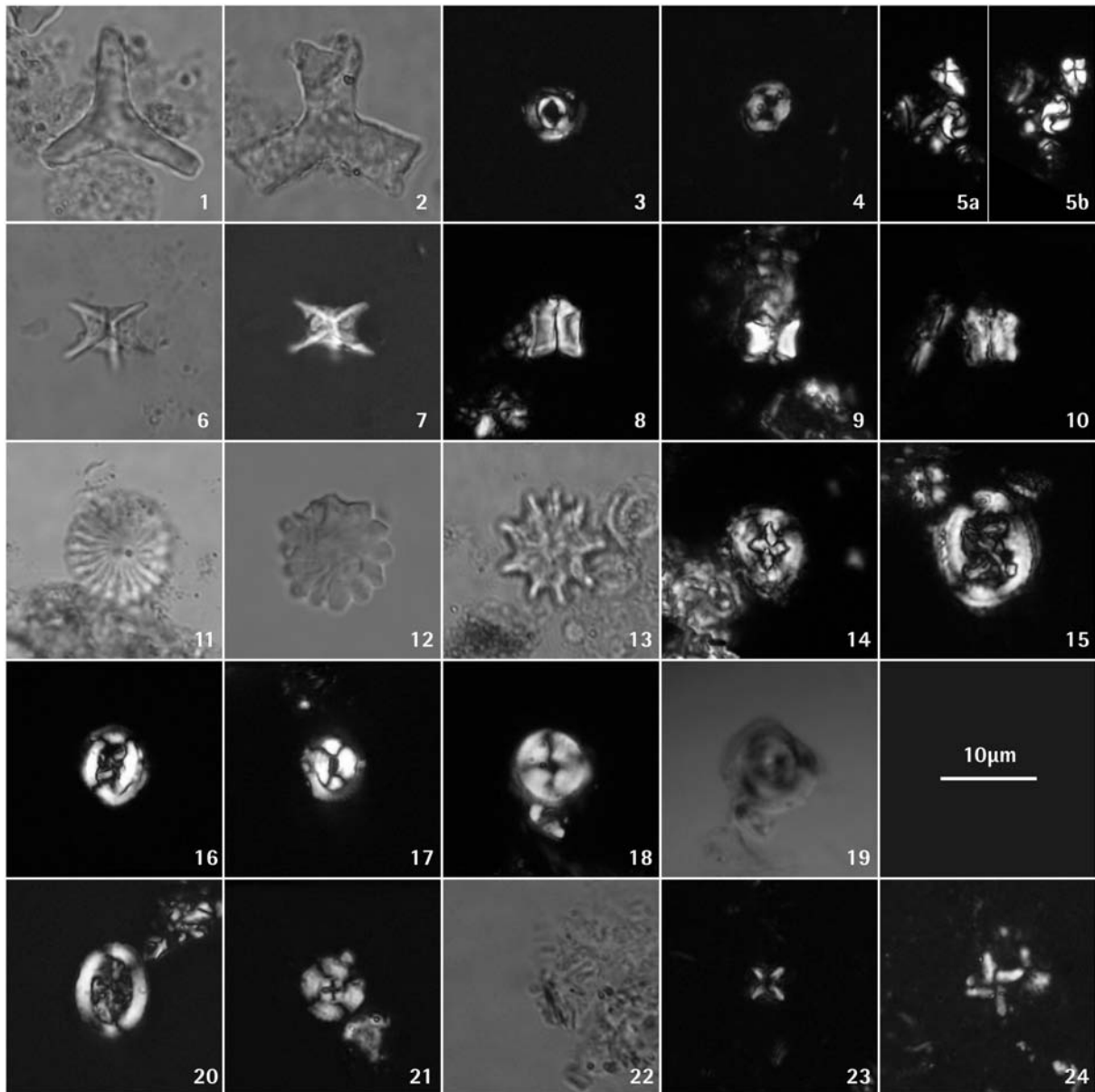


Figure A2.24 ▲

Calcareous nannoplankton from the Goppling section.

Paleogene species: **1** *Tribrachiatus orthostylus* - Gstetten18/09; **2** *Tribrachiatus digitalis* – Gstetten10/09; **3** *Toweius callosus* – Gstetten22/09; **4** *Toweius occultatus* - Gstetten22/09; **5 a and b** *Sphenolithus anarrhopus* – Achthal 12/09; **6 and 7** *Rhomboaster cuspis* – Gstetten22/09; **8** *Fasciculithus tympaniformis* – Achthal12/09; **9** *Fasciculithus billii* – Achthal28/09; **10** *Fasciculithus ulii* – Achthal28/09; **11** *Discoaster multiradiatus* – Gstetten13/09; **12** *Discoaster mohleri* - Achthal12/09; **13** *Discoaster falcatus* - Gstetten13/09; **14** *Cruciplacolithus tenuis* – Achthal12/09; **15** *Chiasmolithus bidens* – Achthal12/09; **16** *Chiasmolithus danicus* - Achthal12/09; **17** *Coccolithus pelagicus* - Achthal12/09; **18 and 19** *Bomolitus elegans* - Achthal28/09.

Maastrichtian: **20** *Arkhangelskiella cymbiformis* - Achthal18/09; **21** *Ceratolithoides cf. kamptneri* - Achthal18/09; **22** *Cyclagelosphaera reinhardtii* - Achthal18/09; **23** *Micula staurophora* - TS10/09; **24** *Micula prinsii* - TS10/09.

The deep-water system of the Achthal Formation is interpreted to have initially filled a slope depression lying above a subsiding basement fault block. Initial subsidence occurred in the latest Maastrichtian and continued into the early Paleogene. Synsedimentary tectonic activity was the primary control on the depositional evolution of the slope-basin.

In the forest south of Teisendorf and Oberteisendorf, a number of small creeks have created excellent exposures of the Achthal Formation. Almost all such outcrops lie to the south of the hiking trail running between the two villages. For better orientation, the more important creeks have been numbered (Fig. A2.21). The Ultrahelvetic nappe complex in the area is composed of three tectonic slices exposing beds con-

tinuously dipping to the southeast. During the field trip we will see part of the ca. 320 m thick sedimentary succession of the Goppling slice, which comprises Maastrichtian to lower Eocene deposits (Fig. A2.22).

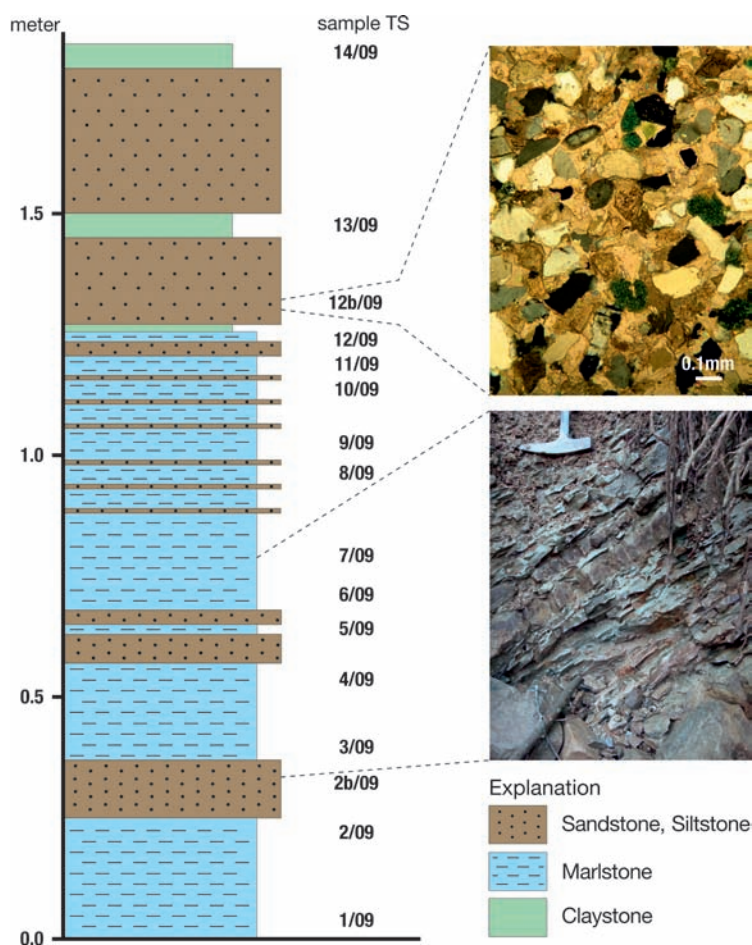
STRATIGRAPHIC FRAMEWORK OF THE GOPPLING SECTION

Maastrichtian

The basal part of the Goppling section is formed by ca. 50 m of bioturbated red clayey marlstone, which is assigned to the Buntmergelserie. The top of this red-bed succession is exposed in creek 3 ("Goppling creek"), immediately south of the hiking trail bridge (Fig. A2.23/1). There, the marlstone contains 19 wt% carbonate. The nannoplankton assemblages are dominated by *Micula staurophora*, whereas all other species are rare and most specimens are preserved only as fragments. Apart from *Lithraphidites quadratus*, the zonal marker for the upper Maastrichtian Zone CC25, *Arkhangelskiella cymbiformis* (Fig. A2.24/20), *Cyclagelosphaera reinhardtii* (Fig. A2.24/22), *Eiffellithus turriseiffeli*, *Micula staurophora*, *Prediscosphaera cretacea*, *Retecapsa crenulata*, and *Watznaueria barnesae* occur. At the top of the red marlstone outcrop, small specimens of *Ceratolithoides cf. kamptneri* were observed (Fig. A2.24/21), indicating already Zone CC26.

Two samples for foraminifera studies were taken from the red marlstone at the outcrop in creek 3 outcrop. The assemblages consist essentially of a rich agglutinated fauna and a small number of calcareous benthic species. Very small planktic species were found only in one sample and display excellent grain-size sorting suggesting reworking by current activity.

Predominant dissolution-resistant species in the calcareous nannoplankton assemblages and the composition of foraminifera assemblages indicate sedimentation of the Maastrichtian red clayey marlstone in a deep-water environment. The absence of an autochthonous planktic fauna indicates deposition below the foraminiferal lysocline, where all planktic foraminifera are dissolved. Below the lysocline and above the calcite compensation depth (CCD) calcareous nannoplankton form coccolith ooze, because in spite of their small size, some coccoliths are more dissolution-resistant than foraminifera (see Hay, 2004, for a review).



In the latest Maastrichtian (*Micula prinsii*-Zone), rapid subsidence brought the Ultrahelvetic sea-floor to below the CCD. The red marlstone transitionally passes into ca. 5 m of grey marlstone with intercalated thin carbonate-cemented parallel-laminated turbiditic siltstone and sandstone beds (Fig. A2.25). The best outcrop of these rocks was found in creek 2 about 10 m south of the hiking trail. In the lower part of this out-

Figure A2.25 ◀

Log of the upper Maastrichtian (*Micula prinsii*-Zone) in the creek 2 section. The lower photograph shows grey to pale red marlstone displaying carbonate contents of ca. 20 wt% and intervening calcite cemented fine-grained turbiditic sandstone beds. The upper photograph is the image of a thin-section of such a sandstone. Calcite replacement affected the components (predominantly single-crystal quartz grains displaying straight extinction, small amounts of K-feldspar and glauconite, very rare mica and cherts) and a possible matrix. The composition of the original sandy fraction cannot be assessed due to the strong diagenetic alteration.

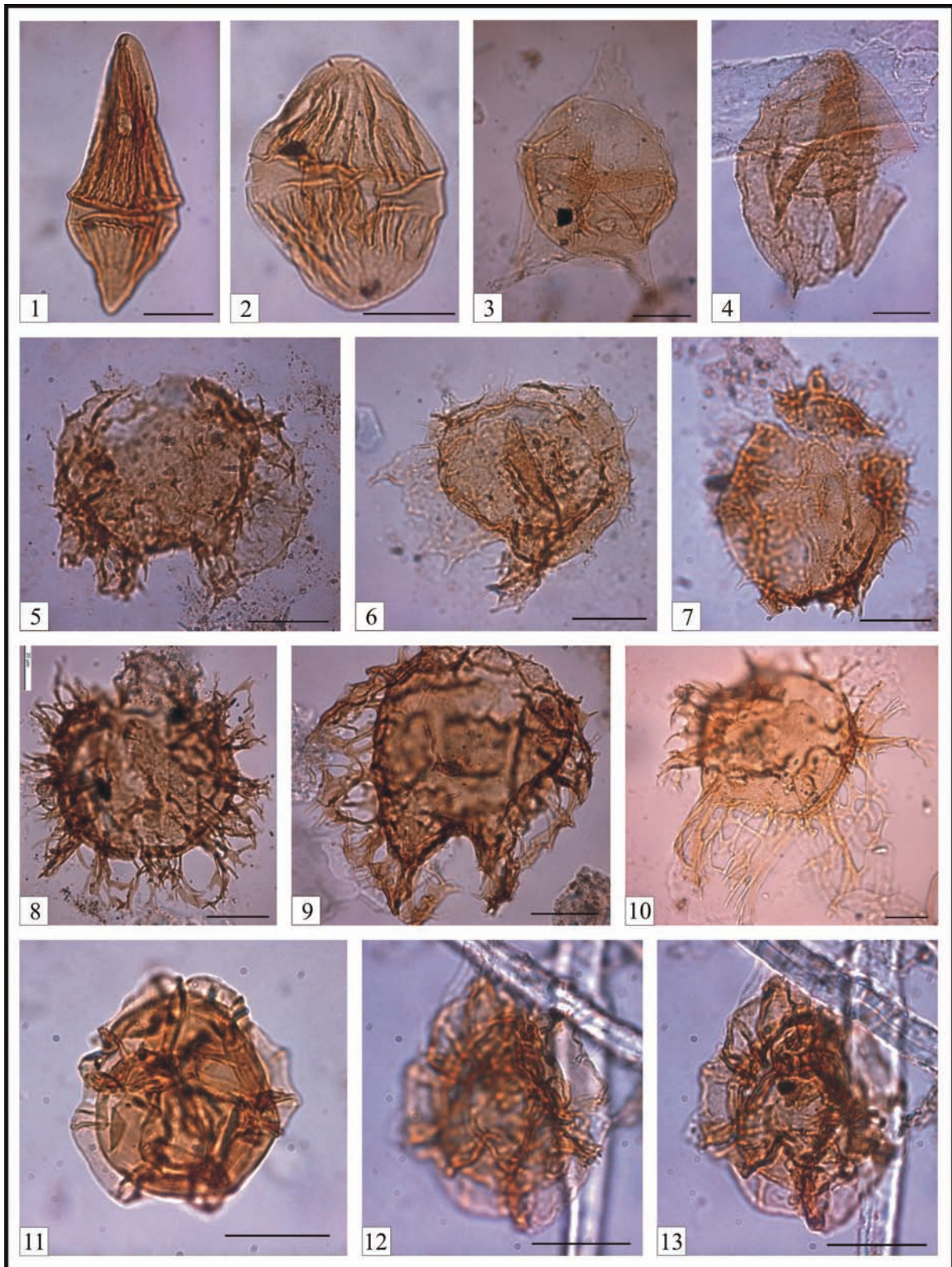


Figure A2.26 ▲

Dinoflagellate taxa from the Goppling section. The species name is followed by sample location and England Finder coordinates (for localization of the specimen on the slide). Scale is 20 µm. **1** *Dinogymnium acuminatum* - TS11/09/a, O24; **2** *Dinogymnium* sp., TS11/09/a, F7/3; **3** *Cerodinium* sp, TS11/09/a, X16/3; **4** *Trithyrodinium* *suspectum* - TS8/09/a, B24/2; **5** *Palynodinium grillator* - TS13/09/a, C40; **6** *Palynodinium grillator* - TS11/09/a, W36; **7** *Palynodinium minus* - TS13/09/b, Y27; **8** *Areoligera volata* - Ach.2/09/a, G12; **9** *Areoligera coronata* - Ach.1/09/a, A3; **10** *Areoligera gippingensis* - TS11/09/a, X34; **11** *Pterodinium cingulatum* subsp. *cingulatum* - TS12/09/a, W33/4; **12** and **13** *Pterodinium aliferum* - TS8/09/a, D6/1.

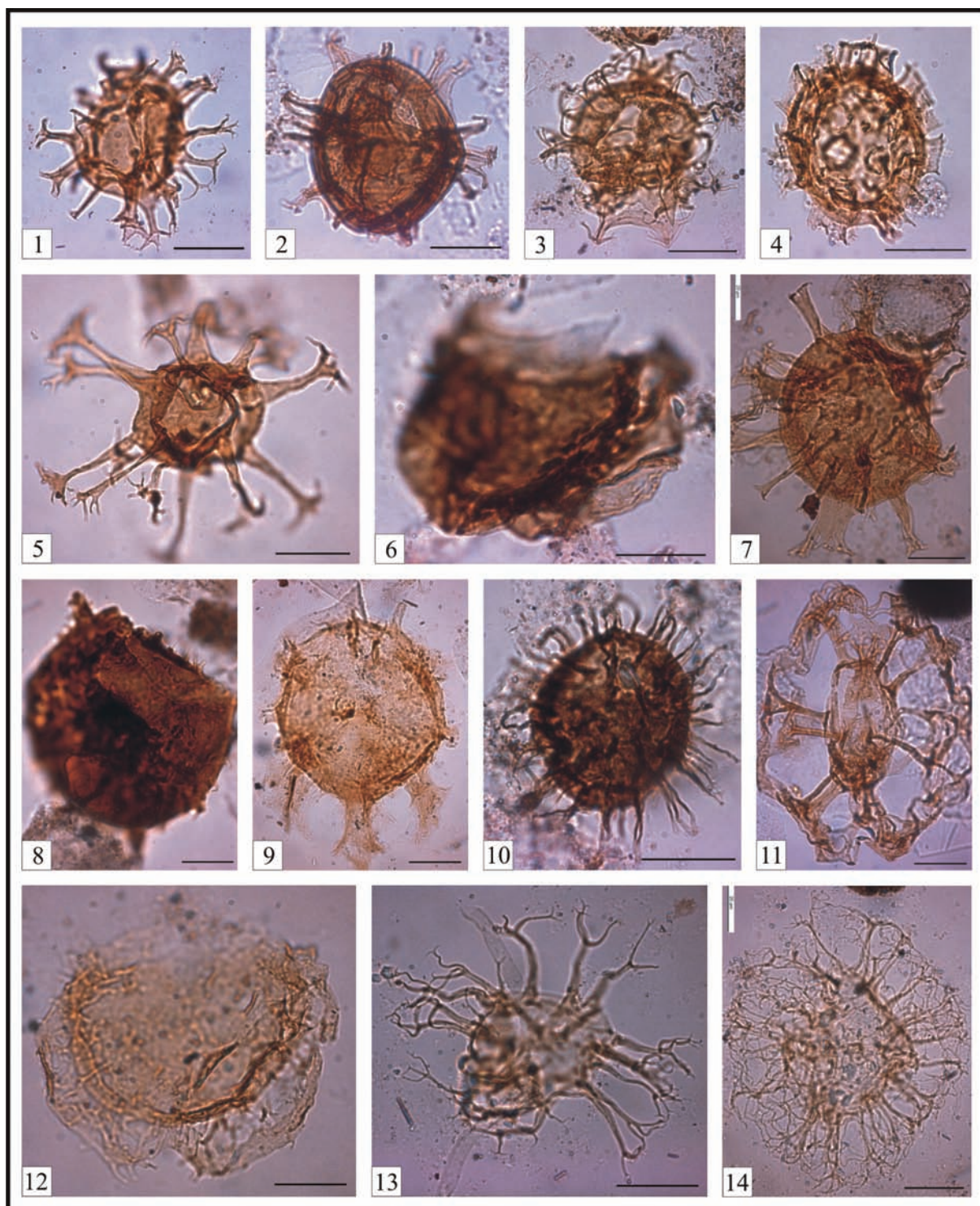


Figure A2.27 ▲

Dinoflagellate taxa from the Goppling section (continuation). The species name is followed by sample location and England Finder coordinates (for localization of the specimen on the slide). Scale is 20 μ m. **1** *Achomosphaera* cf. *alcicornu* - TS13/09/b, N5; **2** *Spiniferites pseudofurcatus* - TS4/09/b, X51/1; **3** *Hystrichostrogylon membraniphorum* - TS12/09/a, N24/2; **4** *Achilleodinium biformoides* - TS11/09/a, X8; **5** *Oligosphaeridium complex* - Ach. 2/09/a, G12; **6** *Senoniasphaera inornata* - Ach. 2/09/b, F40; **7** *Cordosphaeridium fibrospinosum* - TS12/09/a, B36/3; **8** *Carpatella cornuta* - Ach.1/09/b, K16; **9** *Damassadinium californicum* - TS11/09/a, P10; **10** *Operculodinium centrocarpum* - Ach.2/09/b, B25/4; **11** *Rigaudella aemula* - TS4/09/b, D18/1; **12** *Glaphyrocysta perforate* - TS11/09/a, S14/1; **13** *Surculosphaeridium longifurcatum* - TS11/09/a, M46/2; **14** *Trabeculidium quinquetrum* - TS12/09/a, D34/2.

crop, carbonate values of three samples (TS2/09, TS7/09 and TS9/09) range between 20.8 wt% and 21.5 wt%. In the upper part carbonate values decrease to 9.4 wt% (TS10/09) and finally to less than 2 wt% (TS12/09, TS13/09 and TS14/09). Dinoflagellate cyst assemblages indicate a Maastrichtian age of the claystone as in the uppermost sample *Dinogymnium acuminatum* occurs (Fig. A2.26/1), which does not cross the K/Pg-boundary (e.g. Stover et al. 1996).

Associated with this regional subsidence along the southern continental margin of the European Plate, was the onset of turbidite sedimentation. Turbidity currents running parallel with the strike of the slope indicate an opposing topographic high, which caused deflection of the down slope sediment transport (Kneller and McCaffrey, 1999). Subsidence of the sea-floor associated with the deposition of sediment-gravity flows and the coeval generation of a sea-ward bounding topographic high suggest the formation of an intra-slope basin on subsiding crustal fault blocks.

Danian

Danian and Selandian deposits are almost continuously exposed in the Goppling creek gully. Due to the carbonate depletion, no calcareous plankton could be found in the siliciclastic succession, although dinoflagellate assemblages of samples Ach1/09 and Ach2/09 (see Tab. 1 and Fig. A2.27/6, 8 and 9) contain *Carpatella cornuta*, *Damassadinium californicum* and *Senoniasphaera inornata*, which have their first appearance date in the early Danian. *Palynodinium grallator* (Fig. A2.26/5 and 6) has its highest occurrence in the lowermost Danian planktonic foraminiferal Zone P1a (Habib et al., 1996; Dam et al., 1998; Brinkhuis et al., 1998). The samples were taken at the base (Ach1/09) and top (Ach2/09) of the same outcrop (Fig. A2.23/2). Consequently, this outcrop can be assigned to Zone P1a in the zonation of Berggren et al. (1995).

The Danian shows a two-fold lithological subdivision. The 30 m thick lower part is dominated by thin-bedded (< 40 cm) parallel-laminated sandstone turbidites, that rarely show thin capping mudstone (Fig. A2.23/2). In contrast to the Maastrichtian turbidites, the Danian ones are not calcite cemented and do not contain carbonate at all. They are fine-grained (grain diameters up to 0.2 mm), show clast supported fabrics, and have a quartzarenitic composition. Beside quartz (ca. 90% of the grains), feldspar, chert and glauconite occur as components. Freimoser (1972) noted that the heavy mineral assemblages of these Paleocene sandstones are essentially composed of zircon, tourmaline and rutile (together about 90% of the assemblage). Hemipelagic claystone between the turbidite beds is rare and when present only a few millimeters thick indicating that (1) turbidity currents entered the basin with a high frequency and (2) deposition took place below the local CCD.

In the 40 m thick upper part of the Danian, hemipelagic layers are common and often display red colors (Fig. A2.23/3 and 4). Packages of red hemipelagic claystone contain thin base truncated turbiditic siltstone to sandstone beds. These packages are separated by single thick (> 0.5 m) medium to coarse-grained sandstone beds showing grain diameters up to 1.0 mm. As in the lower Danian, only K-feldspar components can be observed and plagioclase is entirely absent. The beds are either massive or show stratification defined by 2–5 cm thick laminae. Graded (Ta) and parallel laminated (Tb) Bouma divisions form the major parts of these beds. Small-sized terrestrial plant remnants are commonly concentrated in horizontal Td-layers near the top of the beds and indicate a derivation of the turbidite material from land areas. Submarine erosion is evidenced by flute casts, which indicate sediment transport predominantly from the west, parallel to the approximately east-west trending slope (Fig. A2.23/5).

One sample (Ach3/09) of the red claystone was studied for dinoflagellates but contained only *Areoligera senonensis*, which has a range from the Cretaceous to the Paleogene. Together with the last red hemipelagites, grey turbiditic clayey marlstones occur, containing strongly corroded nannoplankton assemblages. Beside substantial admixtures of Cretaceous species, *Chiasmolithus danicus*, *Cruciplacolithus tenuis*, *Coccolithus pelagicus* and *Toweius spp.* are indicative for the Danian (*Chiasmolithus danicus* Zone, NP3). However, the absence of *Ellipsolithus macellus*, the zonal marker for Zone NP4, might only be a consequence of the poor preservation in this sample.

Selandian

About 10 m up-section from the above mentioned Danian sample, nannoplankton assemblages contain *Fasciculithus tymaniformis*, the zonal marker for the calcareous nannoplankton Zone NP5 of earli-

est Selandian age. With the disappearance of red hemipelagites the discrimination between turbiditic and non-turbiditic rocks becomes difficult. Single turbidites show a distinct pelitic component (Bouma T_d) in this part of the Goppling section, with approximately the same thickness as the sandy part of the turbidite. This turbiditic mudstone only occasionally contains carbonate. In most cases it is devoid of carbonate and displays the same grey color as the supposed hemipelagic mudstone.

The Selandian, which forms the morphologically steepest part in the course of creek 3, is composed of a ca. 25 m thick thickening and coarsening upward succession. In the lower part of this succession decimeter-scale turbidites occur. Continuing up the exposure, the bed thicknesses gradually increase up to 1.5 m at the top of the succession (Fig. A2.23/6). These sandstone beds are the thickest beds in the entire Achthal Formation and do not display turbiditic mudstone. In part, they contain intraformational mudstone clasts with diameters up to 0.2 m. Flute casts indicate paleotransport from west to east and thus an orientation parallel to the trend of the paleoslope (Fig. A2.28).

Thanetian

In spite of excellent exposures along creek 3, the boundary between the Selandian and Thanetian is difficult to fix precisely due to carbonate depletion and the lack of calcareous plankton. Ca. 20 m downstream from the confluence in the uppermost part of creek 3 (Fig. A2.21), *Fasciculithus billii* is indicative for the upper part of Zone NP5. From here on upstream, a ca. 40 m thick part of the section is characterized by abundant olive-green strongly bioturbated „spotty“ claystone. Probably, the majority of the oval spots in these hemipelagic deposits represent cross sections of the trace fossils *Planolites* and *Thalassinoides* (Uchman, 1999). *Thalassinoides* ispp. and a strongly fragmented specimen of ?*Scolica strozzii* were found also as semi-reliefs at the base of turbidite beds (Fig. A2.29/4, 5 and 6).

The turbidites intervening with the claystone are mostly thin bedded and occasionally display substantial amounts of glauconite, resulting in green rock colors. Glauconite was deformed during burial and flowed around adjacent quartz grains. This is indicated by the patchy distribution of glauconite-filled areas, which are much larger than normal pores.

Some beds show a lenticular shape. The orientation of paleoflow indicators (flute casts and erosional channels) suggest paleotransport from north to south, following the gradient of the south-facing paleoslope (Fig. A2.23/7 and Fig. A2.30). *Discoaster mohleri* (Fig. A2.23/12) indicative of Thanetian zone NP7, was found in the eastern branch of creek 3, about 50 m up-stream from the confluence with the western branch (Fig. A2.21). *Discoaster multiradiatus* (Fig. A2.24/11), the zonal marker of Zone NP9, was found in the uppermost part of the western branch.



Figure A2.28 ◀
Flute casts at the base of a south-dipping bed indicating longitudinal paleotransport from west to east (creek 3)

Ypresian

The Ypresian of the Goppling section shows a two-fold lithological subdivision. The lower part consists of a ca. 50 m thick succession of decimeter-scale turbiditic sandstone and siltstone beds alternating with red colored marly claystone (Fig. A2.23/8). The latter rock is often bioturbated and probably represents hemipelagic non-turbiditic material. As its carbonate values range between 4 wt% and 8 wt%, sedimentation slightly above the CCD can be assumed.

Samples containing *Rhomboaster cuspis* (Fig. A2.24/6 and 7) were found in the lower part of creek 5, about 20 m to the north of the hiking trail. *R. cuspis* has its first appearance date at the Paleocene/

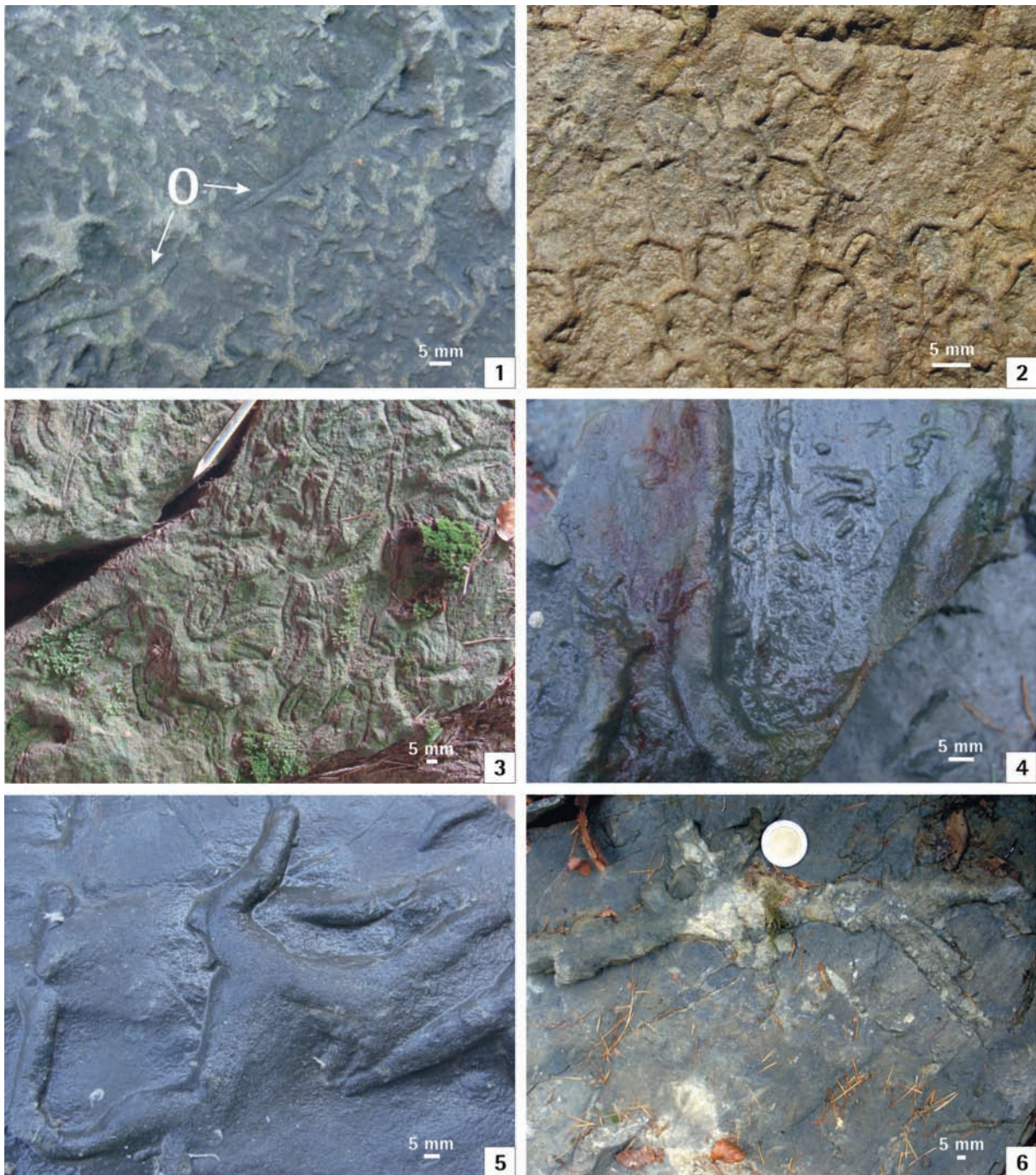


Figure A2.29 ▲

Ichnofossils from the Thanetian (creek 3) and Ypresian (creek 4) of the Goppling section 1) *Ophiomorpha annulata* (O) and ? *Protopaleodictyon* isp. – creek 3; 2) *Paleodictyon majus*.- creek 4; 3) *Scolicia prisca* – creek 4; 4) ? *Scolicia strozzii* – creek 3; 5) *Thalassinoides* isp. – creek 3; 6) *Thalassinoides* isp. – creek 3.



Figure A2.30 ▲

Flute casts at the base of a south-dipping bed indicating transverse paleotransport from north to south (creek 3).

by a fault from the underlying part of the succession in creek 4. In this gully, the topographically lowest outcrops lie just down-stream the hiking trail (Fig. A2.23/8). *T. orthostylus* with pointed rays (Fig. A2.24/1) co-occurs with *Chiasmolithus bidens*, *Coccolithus pelagicus*, *Discoaster barbadiensis*, *D. multiradiatus*, *Ellipsolithus macellus* and *Sphenolithus primus*. Whereas the robust and dissolution resistant *Tribrachiatulus* specimens may be common in the samples, the other species, in particular the discoasterids, are exceedingly rare due to dissolution. Carbonate values of two samples from this outcrop were 4.2 wt% and 4.8 wt%.

A few meters up-stream from the hiking trail the red bed facies in creek 4 shows a sharp sedimentary contact to an overlying ca. 60 m thick sand-rich and thin-bedded turbidite succession that displays only rare and very thin carbonate depleted hemipelagic layers. This suggests that the upper part of the Ypresian succession was deposited below the CCD and hence another subsidence pulse can be assumed. This interpretation is supported by the orientation of flute casts, which indicate paleoflow directions from west to east.

This part of the Goppling section commonly contains trace fossils (e.g. *Paleodictyon majus* and *Scolicia prisca*, see Fig. A2.29/2 and 3). According to Uchman (1999) the ichnogenus *Paleodictyon* probably reflects a moderate shortage of food. These generally oligotrophic conditions were interrupted by periodic accumulation of organic detritus (e.g. plant detritus) by turbidity currents. These more eutrophic episodes favored the ichnogenera *Ophiomorpha* and *Scolicia*. In the Rhenodanubian Group (Egger and Schwerd, 2008) of the adjacent abyssal Penninic basin, the ichnogenera *Ophiomorpha*, *Paleodictyon* and *Scolicia* are known exclusively from the Greifenstein Formation of Eocene age (Uchman, 1999).

DEPOSITIONAL EVOLUTION

Due to the lack of information about the three-dimensional geometry of the basin-fill, the scale and shape of this basin is unknown. It can be assumed that it was a narrow elongate, structurally controlled depression where tectonic activity was the primary control on sedimentation. Presumably, this confined basin was too small for the development of a large-scale deep-sea fan. Instead a channelized deep-water system could be expected, with the bounding slopes of the basin acting as channel walls (Fig. A2.31). Gravity-induced flows entering a sub-basin drop their sediment load and prograde across the depression forming a thickening and coarsening upward succession (Anderson et al., 2006; Shultz and Hubbard, 2005).

At the front of this prograding lobe-like body the thin-bedded sand-rich turbidite succession of early Danian age was deposited (e.g. Crabaugh and Steel, 2004). The lack of muddy tops can be interpreted as an effect of flow-stripping of the fine-grained component of the turbidity currents (e.g. Piper and Normark, 1983; Sinclair and Tomasso, 2002). This indicates that during this early stage of basin evolution,

Eocene-boundary, which is situated in the upper third of Zone NP9. About 25 m to the south of the hiking trail, *Tribrachiatulus digitalis* (Fig. A2.24/2) occurs, the marker fossil of sub-Zone NP10b in the refined zonation scheme of Aubry (1992). About 15 m further up-section, another outcrop of the red bed facies occurs and provided *Tribrachiatulus orthostylus* (Fig. A2.24/1), whereas *T. contortus*, which has its highest occurrence at the NP10/NP11-boundary is absent. Therefore these samples can be assigned to the lower part of NP11 (*Discoaster binodosus*-Zone). Thus, in summary, the red bed facies encompasses the upper part of NP9 to the lower part of NP11.

Along strike to west, red beds containing *R. cuspis* were found in the upper part of creek 4. These deposits are separated

the confining sill was still low. Hence it could be surmounted by the lower-density fraction of the turbidity currents, while the coarse-grained higher density portions of the flows were deflected and preserved upstream of the barrier. The rare and thin hemipelagites indicate the existence of high-frequency trigger mechanisms (e.g. earthquakes) for turbidity currents during the onset of basin formation.

In a conventional fan model, the upper Danian packages of thin-bedded turbidites and red hemipelagic mudstone, which are separated by single thick sandstone beds, can be interpreted as interchannel deposits. In such a model, the thin-bedded turbidites are thought to result from low-density currents overflowing adjacent active channels, while the thicker beds are explained as the result of crevasses in the channel levee, which let high density turbidity currents (Lowe, 1982) escape to the basin floor (e.g. Mutti, 1977). This model implies the existence of subordinate fairways within the slope-basin.

Alternatively, the upper Danian facies can be seen as the result of an episode of comparatively tectonic quiescence. Siliciclastic material accumulated at the shelf edge over time and larger turbidity currents triggered by earthquakes or gravity load entered the slope-basin with low periodicity. This is indicated by the common occurrence of intervening hemipelagic red claystone as their deposition indicates very low sedimentation rates. The lack of muddy tops of the thick-bedded turbidites can again be explained as a result of flow-stripping as flow thickness was determined as the primary control of the run-up distance of a turbidity current onto the opposing slope (Muck and Underwood, 1990). It is assumed, that high-density currents (Lowe, 1982) lost their fine-grained component by down-spill, so that only their coarse-grained material is preserved in the sub-basin. Low-density currents had not the potential to surmount the bounding slope and remained completely in the sub-basin.

Increased subsidence at the end of the Danian caused ponding of the turbidity currents, which display a distinct pelitic component. However, sedimentation rates quickly outpaced subsidence rates and deposition reduced the relief sufficiently to allow spill down-slope. The filling up of the basin to the spill-point is indicated by downslope paleotransport directions in the upper Selandian and Thanetian. Due to the gradient reduction in the area of the former basinal structure turbidites were deposited on this flat surface and the ca. 95 m thick basin-fill succession of Danian and Selandian age became buried by slope deposits developing into a healed slope (e.g. Smith, 2004).

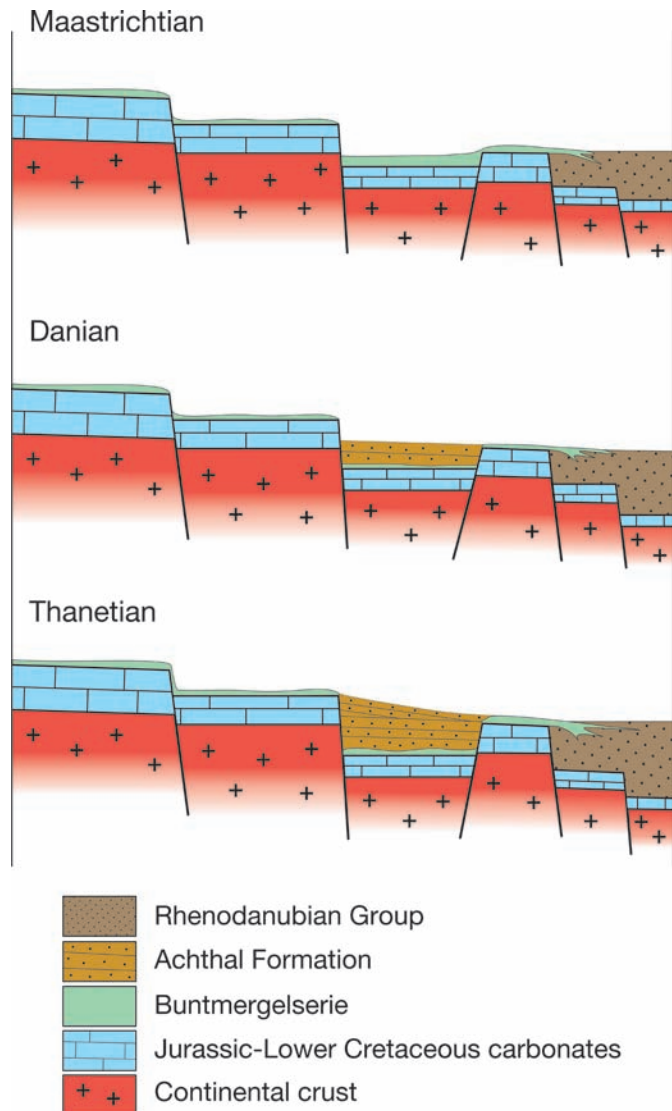


Figure 11 ▲
Slope basin model for the deposition of the Achthal Formation.